

Research Article

Morphology and Mechanical Properties of 3D Porous PLA/PCL Scaffolds

M. Dolatkhahan, M. Peiravi and Z. Sherafat*

Department of Materials Science and Engineering, School of Engineering, Shiraz University, Shiraz, Iran

ARTICLE INFO

Article history:

Received 28 September 2024

Reviewed 27 October 2024

Revised 29 October 2024

Accepted 3 November 2024

Keywords:

Polycaprolactone

Polylactic acid

Solvent casting/particle leaching

Bone tissue engineering

Please cite this article as:

Dolatkhahan, M., Peiravi, M., & Sherafat, Z. (2024). Morphology and mechanical properties of 3D porous PLA/PCL scaffolds. *Iranian Journal of Materials Forming*, 11(3), 21-27. <https://doi.org/10.22099/ijmf.2024.51296.1305>

ABSTRACT

The fabrication and evaluation of tissue engineering scaffolds is a new research field with significant applications in medicine. Various polymers have been considered for the fabrication of bone scaffolds due to their biocompatibility, biodegradability, and excellent mechanical properties. Polycaprolactone and polylactic acid are both biodegradable and biocompatible polymers; however, polylactic acid is brittle, and polycaprolactone is hydrophobic, which reduces cell adhesion on the surface. Therefore, combining these two polymers may be an effective approach to developing a new biomaterial. In this study, PLA/PCL scaffolds with different PLA/PCL weight ratios were fabricated using the solvent casting/particle leaching method. To evaluate the morphology, wettability, and mechanical properties of the scaffolds, scanning electron microscopy (SEM), a contact angle goniometer, and compression and tensile tests were used, respectively. SEM images of the samples showed that all the samples have porosity ranging from 70 to 85%, with pore sizes of 250 to 500 micrometers, which is suitable for cell infiltration, proliferation, and growth. Contact angle measurements indicated that the presence of PLA increased the hydrophilicity of composite samples. PCL/PLA samples have lower ductility and higher stiffness than pure PCL. However, the weak interface between PLA and PCL resulted in some composite samples having lower strength than pure PCL. The PCL/PLA scaffold shows promise as a candidate for bone tissue engineering.

© Shiraz University, Shiraz, Iran, 2024

1. Introduction

Bone grafting is one of the most common surgical procedures for bone regeneration in orthopedic procedures. However, it is a very expensive procedure that can lead to complications at the donor site, such as damage, disability, disfigurement, and scarring. It also carries surgical risks including bleeding, inflammation,

infection, and chronic pain [1]. To address these limitations, the development of bone graft substitutes (BGS) has emerged as one of the most promising solutions in orthopedics [2]. Bone tissue engineering (BTE) uses scaffolds, cells, and growth factors to create artificial bones for implantation in patients [3].

Scaffolds play an important role in bone tissue

* Corresponding author

E-mail address: zsherafat@shirazu.ac.ir (Z. Sherafat)<https://doi.org/10.22099/ijmf.2024.51296.1305>

engineering. Their purpose is to mimic the function and structure of the natural bone extracellular matrix (ECM) by providing a three-dimensional (3D) environment that promotes adhesion, proliferation and differentiation, while also possessing sufficient physical properties for bone repair. An ideal scaffold should be biodegradable, biocompatible, bioactive, bone conductive and bone inductive [4].

Various artificial and natural, biodegradable and non-biodegradable materials have been used in the fabrication of bone scaffolds, including polymers, ceramics, metals and composites. Each of these materials has unique surface activity and biocompatibility, which influence bone induction and conduction [5]. Polymers are widely used as scaffolds due to their biocompatibility, excellent mechanical properties, low risk of allergic reactions, favorable enzymatic responses for cell growth and controlled biodegradation rate [6]. Polycaprolactone (PCL), polylactic acid (PLA), polyglycolide (PGA), poly-L-lactic acid (PLLA) and polyvinylidene fluoride (PVDF) are biocompatible polymers used in tissue engineering [3, 7, 8].

Polycaprolactone is a semi-crystalline linear polyester and is one of the most well-known synthetic polymers in bone tissue engineering. This polymer's characteristics include a very low glass transition temperature ($T_g = -60\text{ }^\circ\text{C}$), low melting point ($59\text{-}64\text{ }^\circ\text{C}$), biocompatibility, biodegradability, high toughness, favorable mechanical strength, good processability, high permeability for various drugs, and high hydrophobicity [9, 10]. PLA, an aliphatic polyester, is used in various fields, including the pharmaceutical industry, biomedicine and food packaging. Its properties include biocompatibility, biodegradability, a glass transition temperature of $60\text{ }^\circ\text{C}$, a melting point of $160\text{ }^\circ\text{C}$, processability, high strength and low flexibility [7, 11-13].

PLA and PCL have been approved by the US Food and Drug Administration (FDA) for use in medical applications such as scaffolds in tissue engineering [3]. Although both polymers are biocompatible and biodegradable, neither is an ideal scaffold for bone tissue

engineering. PCL's hydrophobicity reduces cell adhesion, and PLA is brittle. Therefore, a composite of these two polymers offers an effective option for developing a new biomaterial with favorable mechanical and biological properties [14, 15].

There are various methods for the fabrication of scaffolds; the most common include phase separation, gas foaming, solvent casting/particulate leaching, freeze drying, electrospinning, and 3D printing [16]. Among these, the solvent casting/particulate leaching technique is a widely used method for producing polymer-based scaffolds. In this technique, the polymer is dissolved in a suitable solvent, then mixed with an insoluble salt. Evaporation of the solvent produces a salt-polymer composite, which is subsequently washed to remove the salt particles and porosity in place of the salt. The solvent casting/particulate leaching method is relatively simple and does not require specialized or expensive equipment. In addition, it allows for control over the final porosity and pore size, producing a three-dimensional structure similar to the bone matrix [17]. This method is mostly used for cartilage and bone tissue engineering applications, with scaffold porosity ranging from 50 to 90 percent [6].

Electrospun nanofibrous scaffolds with different weight ratios of PCL/PLA (i.e., 0.100, 40.60, and 80.20) were fabricated through thermally induced self-agglomeration of nanofibers (TISA). The results showed that all 3D scaffolds were flexible and had interconnected pores with a size of $300\text{ }\mu\text{m}$. Among them, PLA80 scaffolds demonstrated the best overall properties in terms of density, porosity, water absorption capacity, mechanical properties, bioactivity and cell viability [18]. Additionally, 3D porous scaffolds composed of different ratios of PCL and PLLA were prepared using the salt leaching method for bone regeneration applications. The addition of PLLA increased the porosity, pore size and compressive strength of the scaffold, while also the biocompatibility of the samples was improved by increasing the PLLA content [18]. PCL/PLA/ZnO scaffolds were fabricated using melt extrusion 3D printing. The printed scaffolds had a regular structure with pore sizes between 300 and

400 μm . By adding PLA to PCL, the stiffness increased from 52 MPa to 214 MPa [19].

Considering the potential of PLA/PCL composites as bone scaffolds, the fabrication of this composite using the solvent casting/particulate leaching method has received less attention, despite the method's simplicity, low cost, and ability to produce a 3D structure. The purpose of this research was to fabricate a PLA/PCL composite scaffold using the solvent casting/particulate leaching method to create a 3D structure that mimics the bone extracellular matrix and to investigate its morphology, as well as its physical and mechanical properties.

2. Experimental Procedures

2.1. Materials and methods

To fabricate PLA/PCL composites, polylactic acid (Hisun, REVODE190 (L130)) and polycaprolactone (Aldrich with an average MW of 80,000 Da) were used as the primary materials. Chloroform (Merck) with a purity of 99% served as the solvent, and sodium chloride with a particle size of 250 to 500 microns (Arvin Shimi) was utilized as a porogen.

A 12 wt.% solution of PLA and an 18 wt.% solution of PCL in chloroform were prepared separately at 60 °C. Two solutions were then blended with PLA/PCL weight ratios of 0/100, 25/75, 50/50, 75/25, and 100/0 and stirred at 60 °C for 2 hours to achieve a uniform mixture. Next, sodium chloride was added as a porogen to the polymer mixture at a polymer/salt ratio of 1:8 to create porosity. The resulting mixture was poured into a cylindrical silicone mold with a diameter and height of 11 and 15 mm, respectively. The samples were dried at room temperature for 24 h, after which they were immersed in DI water for 72 hours to dissolve and remove the salt particles, thereby creating porosity. Finally, the samples were dried at 40 °C.

2.2. Characterization

The morphology of the composites was investigated using scanning electron microscopy (TESCAN-Vega 3). The porosity percentage of the samples was measured by

the liquid displacement method, as shown in Eq. (1):

$$\% \text{Porosity} = (V1/(V1+V2)) \times 100 \quad (1)$$

In this equation, V1 represents the volume of sample porosity, calculated by measuring the volume of liquid filling the pores after immersion in ethanol. This volume is determined by the difference between the wet and dry weight of the sample, divided by the density of the liquid. V2 represents the true volume of the scaffold, obtained by dividing the dry weight by the theoretical density of the sample. The PLA/PCL interactions in composite samples were evaluated using Fourier transform infrared spectroscopy (FTIR) (Tensor II, Bruker, Germany) within the 400–4000 cm^{-1} range. The wettability of the samples was assessed using a contact angle goniometer and tensiometer (CAG10, Jikan, Iran). Cylindrical samples with an initial height-to-diameter ratio of 1 and dogbone samples, prepared according to the ASTM D638 standard, were prepared for compression and tensile tests, respectively. The mechanical properties of the samples were assessed using a tensile test instrument (SANTAM, Iran) at a crosshead speed of 10 mm/min.

3. Results and Discussion

The pore structure of the scaffolds was evaluated using SEM images. Fig. 1 presents the electron micrographs of the fracture surface of the fabricated samples. As shown, all samples exhibit continuous and uniform porosities, achieved by removing the salt. The pore sizes are proportional to the size of the salt used, ranging from 250 to 500 micrometers. The pores are interconnected, and the pore distribution is relatively uniform. The size and geometry of the pores play a critical role in cell infiltration within the scaffolds. Generally, in scaffolds with pore sizes between 80 and 190 micrometers, cell accumulation was observed and proper cell infiltration did not occur. A pore size of at least 300 micrometers is necessary for effective cell infiltration, and the sample porosity provides sufficient space for cell infiltration, proliferation, and growth [19].

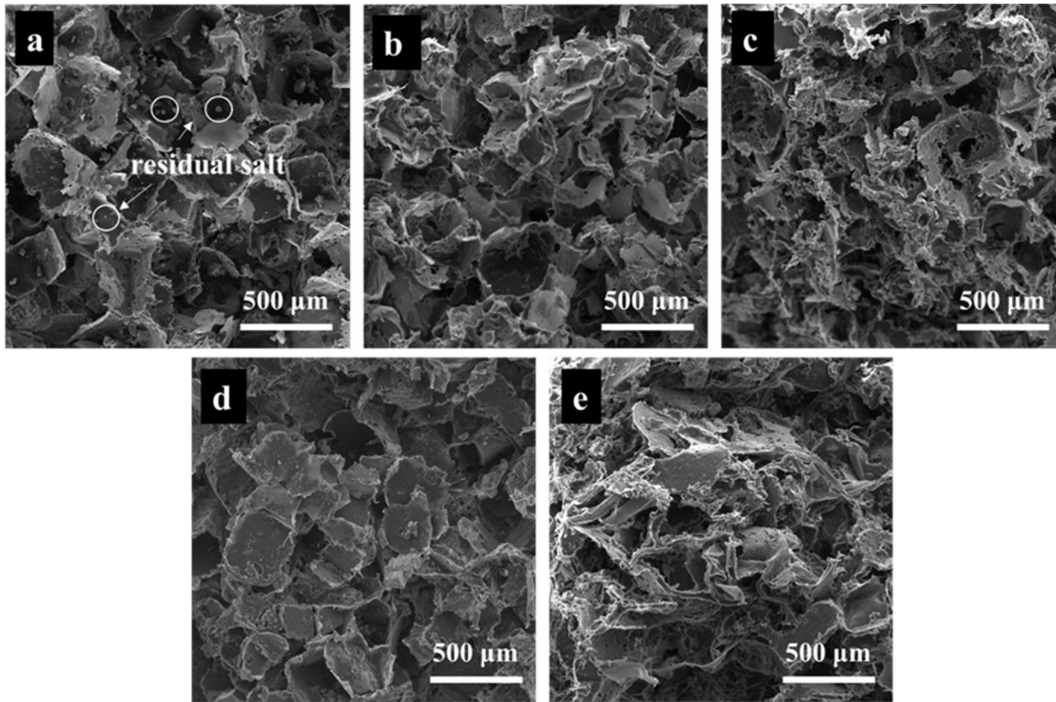


Fig. 1. SEM images of scaffolds with different PLA/PCL compositions: (a) PLA, (b) 75PLA-25PCL, (c) 50PLA-50PCL, (d) 25PLA-75PCL, and (e) PCL.

The porosity of PLA/PCL scaffolds was calculated using the solvent displacement method, and the results are reported in Table 1. The porosity of the samples ranges from 70% to 85%, which, except for the PLA sample, aligns closely with the theoretically calculated porosity based on the amount of salt used. This suggests that all the salts have been dissolved, resulting in the intended porosity. In the PLA sample, due to its hardness, inherent brittleness, and lack of flexibility, it is more challenging to remove the salt completely, leading to reduced porosity. Residual salt particles that are not fully dissolved can be observed in the SEM images. The porosity percentage of the samples is suitable for cell migration and penetration within the scaffold structure.

The FTIR spectra of PLA, 50PLA-50PCL, and PCL samples are shown in Fig. 2. In the PCL spectrum, the bands at 582, 1166, 1721, 2876 and 2953 cm^{-1} correspond to C=O wagging, C-O stretching, C=O stretching, and symmetric and asymmetric CH_2 stretching vibrations, respectively, and are characteristic bands of PCL. In the PLA spectrum, the bands at 1746, 2995, 2946 and 1080 cm^{-1} are associated with C=O

stretching, asymmetric and symmetric CH_3 stretching, and C-O stretching vibrations, respectively. The bands at 1452 and 1361 cm^{-1} are due to asymmetric and symmetric CH_3 bending vibrations. As no new bonds are formed in the composite sample, confirming the lack of interaction between PLA and PCL, the two polymers are immiscible.

The increase in hydrophilicity enhances cell adhesion on the surface of the scaffold. Therefore, the hydrophilicity of PLA/PCL scaffolds was evaluated, and the water contact angle of the samples is shown in Fig. 3. As illustrated, PCL is more hydrophobic than PLA, and the presence of PLA in composite scaffolds reduces the contact angle to some extent, which can improve cell adhesion on the scaffold.

Table 1. The porosity percentage of pure PLA and PCL, and their blended scaffolds

Sample	Porosity (%)
PLA	70
75PLA-25PCL	84
50PLA-50PCL	85
25PLA-75PCL	76
PCL	80

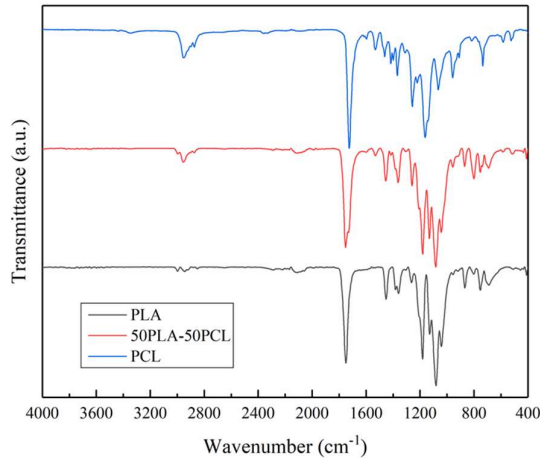


Fig. 2. FTIR spectra of PLA, 50PLA-50PCL, and PCL.

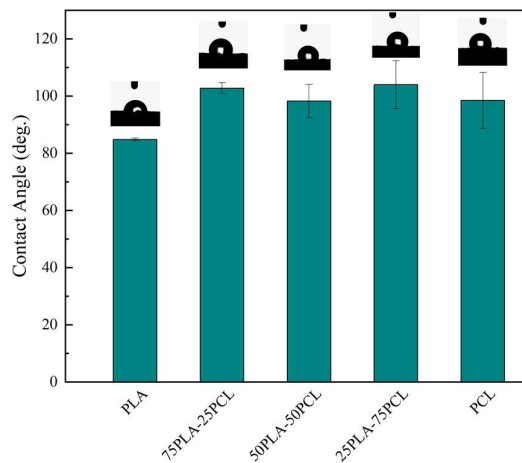


Fig. 3. Water contact angle of pure PLA, pure PCL, and their blended scaffolds.

The mechanical properties of the samples were investigated. For the compression test, cylindrical samples with a diameter of 11 mm and a height ranging from 11 to 14 mm were prepared. The resulting engineering stress-strain curves are shown in Fig. 4. The stress-strain curves of the porous composite scaffolds exhibit foam-like behavior, characterized by three distinct regions: linear elastic deformation at low strains, a plateau region at higher strains, and a densification region at high strains. The stiffness (slope of the elastic region), onset strain of the densification region, and pore wall fracture stress were calculated, and the results are provided in Table 2. As shown, the PLA sample exhibits significantly higher stiffness than the PCL sample. Consequently, stiffness increases in the composite samples as the amount of PLA increases. Comparing the

onset strain of the densification region and the pore wall fracture stress shows that with an increase in PLA content, the onset strain decreases while the strength of the pore walls increases, which is expected given the higher strength of PLA compared to PCL. Only the 50PLA-50PCL sample does not follow this trend, as it has the lowest pore wall fracture stress. The reduced pore wall strength of the 50PLA-50PCL sample can be attributed to the weak interface between PLA and PCL. If the polymer mixture is miscible, a strong interface forms between two polymers; however, if the mixture is immiscible, the interface between the polymers is weak. Based on the FTIR results, no interaction was observed between the PLA and PCL polymers, indicating that these two polymers are immiscible. Miscible mixtures are typically clear, while immiscible mixtures are cloudy, and the cloudiness of the PLA and PCL mixture further supports their immiscibility. Therefore, due to the weak interface between the two polymers, their mixture exhibits lower strength than the pure samples. The 50PLA-50PCL sample has the lowest wall strength, likely due to the larger interfacial area between the polymers.

Table 2. Stiffness, onset strain of the densification region, and wall fracture stress of each scaffold

Sample	Slope of first region (MPa)	Onset strain of the densification region (ϵ_d)	The pore wall fracture stress (σ_d)
PLA	12.17	0.62	2.07
75PLA-25PCL	5.9	0.63	1.17
50PLA-50PCL	1.6	0.67	0.94
25PLA-75PCL	1.62	0.64	1.05
PCL	0.44	0.66	0.87

To evaluate the tensile properties, a tensile test was performed on PCL, PLA and PLA/PCL composite samples. The engineering stress-strain curves of these samples are shown in Fig. 5. Stiffness, ultimate strength and elongation of the samples were calculated, and the results are provided in Table 3. As shown, stiffness increases and elongation decreases with increasing PLA content. Although it is expected that tensile strength would increase with a higher PLA content, the strength

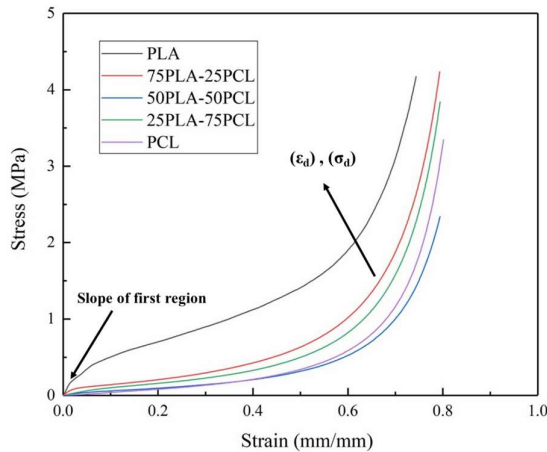


Fig. 4. Compressive stress-strain curves of pure PLA, pure PCL, and their composite scaffolds.

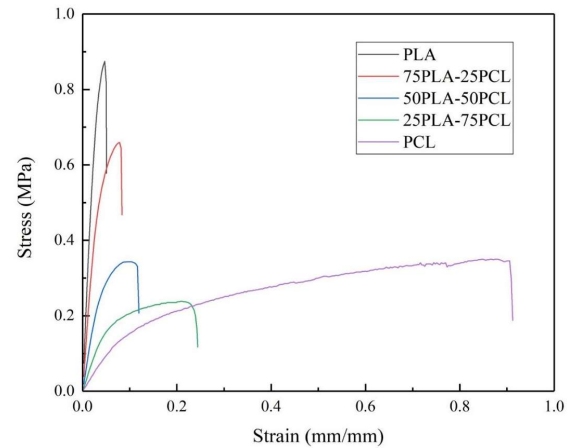


Fig. 5. Tensile stress-strain curves of pure PLA, pure PCL, and their composite scaffolds.

Table 3. Stiffness, tensile strength, and elongation of each scaffold

Sample	Stiffness (MPa)	Tensile strength (MPa)	Elongation (%)
PLA	30.01	0.87	5
75PLA-25PCL	18.17	0.66	8.3
50PLA-50PCL	8.17	0.34	12
25PLA-75PCL	3.55	0.24	24
PCL	1.82	0.35	90

of the 25PLA-75PCL and 50PLA-50PCL composite samples is lower than that of pure PCL. This can be attributed to the immiscibility of the two polymers and the resulting weak interface between them, which reduces the mechanical strength of the scaffold. It can be concluded that in composite samples with a lower amount of PLA, the weak interface effect outweighs the benefits of PLA, resulting in a composite strength lower than that of pure PCL. Due to alignment issues and manufacturing defects, the compressive modulus of the samples is not equal to the tensile modulus [20]. Given that the Young's modulus of cancellous bone ranges from 0.1 to 1 MPa, the fabricated scaffolds are suitable for use in cancellous bone applications [21].

4. Conclusion

In the present study, PLA/PCL scaffolds with five different PLA/PCL ratios (100/0, 75/25, 50/50, 25/75 and 0/100) and a polymer/salt ratio of 1:8 were fabricated using the solvent casting/particulate leaching method.

The porosity and pore size of the samples ranged from 70 to 85% and 250 to 500 micrometers, respectively, providing sufficient space for cell infiltration, proliferation and growth. The presence of PLA increased the hydrophilicity of the composite samples. Due to PLA's higher strength, the composite samples exhibited greater stiffness and reduced ductility compared to pure PCL. However, the weak interface between PLA and PCL caused some composite samples to have lower strength than pure PCL. Based on mechanical properties and contact angle, the 75PLA-25PCL sample most closely resembles bone tissue.

Conflict of interest

The author declares that there is no conflict of interest in this research.

Funding

This research has not received any funding.

5. References

- [1] Amini, A. R., Laurencin, C. T., & Nukavarapu, S. P. (2012). Bone tissue engineering: recent advances and challenges. *Critical Reviews™ in Biomedical Engineering*, 40(5), 363-408. <https://doi.org/10.1615/CritRevBiomedEng.v40.i5.10>
- [2] Wang, W., & Yeung, K. W. (2017). Bone grafts and biomaterials substitutes for bone defect repair: A review. *Bioactive Materials*, 2(4), 224-247. <https://doi.org/10.1016/j.bioactmat.2017.05.007>
- [3] Fang, R., Zhang, E., Xu, L., & Wei, S. (2010). Electrospun PCL/PLA/HA based nanofibers as scaffold

- for osteoblast-like cells. *Journal of Nanoscience and Nanotechnology*, 10(11), 7747-7751.
<https://doi.org/10.1166/jnn.2010.2831>
- [4] Qu, H., Fu, H., Han, Z., & Sun, Y. (2019). Biomaterials for bone tissue engineering scaffolds: A review. *RSC Advances*, 9(45), 26252-26262.
<https://doi.org/10.1039/C9RA05214C>
- [5] Ghassemi, T., Shahroodi, A., Ebrahimzadeh, M. H., Mousavian, A., Movaffagh, J., & Moradi, A. (2018). Current concepts in scaffolding for bone tissue engineering. *Archives of Bone and Joint Surgery*, 6(2), 90-99. <https://doi.org/10.22038/abjs.2018.26340.1713>
- [6] Suamte, L., Tirkey, A., Barman, J., & Babu, P. J. (2023). Various manufacturing methods and ideal properties of scaffolds for tissue engineering applications. *Smart Materials in Manufacturing*, 1, 100011.
<https://doi.org/10.1016/j.smmf.2022.100011>
- [7] Farzamfar, S., Naseri-Nosar, M., Sahrpeyma, H., Ehterami, A., Goodarzi, A., Rahmati, M., Ahmadi Lakalayeh, G., Ghorbani, S., Vaez, A., & Salehi, M. (2019). Tetracycline hydrochloride-containing poly (ϵ -caprolactone)/poly lactic acid scaffold for bone tissue engineering application: In vitro and in vivo study. *International Journal of Polymeric Materials and Polymeric Biomaterials*, 68(8), 472-479.
<https://doi.org/10.1080/00914037.2018.1466133>
- [8] Perez-Puyana, V., Jiménez-Rosado, M., Romero, A., & Guerrero, A. (2020). Polymer-based scaffolds for soft-tissue engineering. *Polymers*, 12(7), 1566.
<https://doi.org/10.3390/polym12071566>
- [9] Abodunrin, O. D., Bricha, M., & El Mabrouk, K. (2024). Developments in 3D-printed polymeric Materials and Bioactive Materials Integration for Biomedical Applications. In *Reference Module in Materials Science and Materials Engineering*. Elsevier. <https://doi.org/10.1016/B978-0-323-95486-0.00028-4>
- [10] Mateos-Timoneda, M. A. (2009). Polymers for bone repair. In *Bone repair biomaterials* (pp. 231-251). Woodhead Publishing.
<https://doi.org/10.1533/9781845696610.2.231>
- [11] Patrício, T., Domingos, M., Gloria, A., D'Amora, U., Coelho, J. F., & Bártolo, P. J. (2014). Fabrication and characterisation of PCL and PCL/PLA scaffolds for tissue engineering. *Rapid Prototyping Journal*, 20(2), 145-156. <https://doi.org/10.1108/RPJ-04-2012-0037>
- [12] Rodan, G. A. (1992). Introduction to bone biology. *Bone*, 13, S3-S6.
[https://doi.org/10.1016/S8756-3282\(09\)80003-3](https://doi.org/10.1016/S8756-3282(09)80003-3)
- [13] Ning, L., & Chen, X. (2017). A brief review of extrusion-based tissue scaffold bio-printing. *Biotechnology Journal*, 12(8), 1600671.
<https://doi.org/10.1002/biot.201600671>
- [14] Zaroog, O. S., Borhana, A. A., & Perumal, S. S. (2019). Biomaterials for bone replacements: past and present. In *Reference Module in Materials Science and Materials Engineering*. Elsevier. <https://doi.org/10.1016/B978-0-12-803581-8.11442-0>
- [15] Hassanajili, S., Karami-Pour, A., Oryan, A., & Talaei-Khozani, T. (2019). Preparation and characterization of PLA/PCL/HA composite scaffolds using indirect 3D printing for bone tissue engineering. *Materials Science and Engineering: C*, 104, 109960.
<https://doi.org/10.1016/j.msec.2019.109960>
- [16] Hutmacher, D. W. (2001). Scaffold design and fabrication technologies for engineering tissues—state of the art and future perspectives. *Journal of Biomaterials Science, Polymer Edition*, 12(1), 107-124.
<https://doi.org/10.1163/156856201744489>
- [17] Sola, A., Bertacchini, J., D'Avella, D., Anselmi, L., Maraldi, T., Marmioli, S., & Messori, M. (2019). Development of solvent-casting particulate leaching (SCPL) polymer scaffolds as improved three-dimensional supports to mimic the bone marrow niche. *Materials Science and Engineering: C*, 96, 153-165.
<https://doi.org/10.1016/j.msec.2018.10.086>
- [18] Xu, T., Yao, Q., Miszuk, J. M., Sanyour, H. J., Hong, Z., Sun, H., & Fong, H. (2018). Tailoring weight ratio of PCL/PLA in electrospun three-dimensional nanofibrous scaffolds and the effect on osteogenic differentiation of stem cells. *Colloids and Surfaces B: Biointerfaces*, 171, 31-39. <https://doi.org/10.1016/j.colsurfb.2018.07.004>
- [19] Peiravi, M., & Sherafat, Z. (2024). Morphology and mechanical properties of 3D printed PCL-PLA-ZnO nanocomposite scaffolds for bone regeneration. *Journal of Ultrafine Grained and Nanostructured Materials*, 57(1), 28-34.
<https://doi.org/10.22059/jufngsm.2024.01.04>
- [20] Meng, M., Le, H. R., Rizvi, M. J., & Grove, S. M. (2015). The effects of unequal compressive/tensile moduli of composites. *Composite Structures*, 126, 207-215.
<https://doi.org/10.1016/j.compstruct.2015.02.064>
- [21] Brydone, A. S., Meek, D., & MacLaine, S. (2010). Bone grafting, orthopaedic biomaterials, and the clinical need for bone engineering. *Proceedings of the Institution of Mechanical Engineers, Part H: Journal of Engineering in Medicine*, 224(12), 1329-1343.
<https://doi.org/10.1243/09544119JEIM770>